Carbohydrate Polymers 292 (2022) 119685

Contents lists available at ScienceDirect

Carbohydrate Polymers

journal homepage: www.elsevier.com/locate/carbpol

Identification of plant polysaccharides by MALDI-TOF MS fingerprinting after periodate oxidation and thermal hydrolysis

Carolina O. Pandeirada [a], Jos A. Hageman [b], Hans-Gerd Janssen [c,d], Yvonne Westphal [c], Henk A. Schols [a,*]

[a] Wageningen University & Research, Laboratory of Food Chemistry, Bornse Weilanden 9, 6708 WG Wageningen, the Netherlands
[b] Biometris, Applied Statistics, Wageningen University & Research, Droevendaalsesteeg 1, 6700 AA Wageningen, the Netherlands
[c] Unilever Foods Innovation Centre — Hive, Bronland 14, 6708 WH Wageningen, the Netherlands
[d] Wageningen University & Research, Laboratory of Organic Chemistry, P.O. Box 8026, 6700 EG Wageningen, the Netherlands

ARTICLE INFO

Keywords:
Plant polysaccharides recognition
Periodate oxidation
Oxidized oligosaccharides
MALDI-TOF MS

ABSTRACT

An autoclave treatment at 121 °C on periodate-oxidized plant polysaccharides and mixes thereof was investigated for the release of oligosaccharides to obtain a generic polysaccharide depolymerization method for polysaccharides fingerprinting. Matrix-Assisted Laser Desorption Ionization Time-Of-Flight Mass Spectrometry (MALDI-TOF MS) analysis of the oligosaccharides released showed that each polysaccharide had a unique oligosaccharides profile, even the same type of polysaccharide derived from different sources and/or having different fine structures (*e.g.* class of (arabino)xylans, galactomannans, glucans, or pectic materials). Various polysaccharide classes present in a polysaccharide mix could be identified based on significantly different ($p < 0.05$) marker *m/z* values present in the mass spectrum. Principal component analysis and hierarchical cluster analysis of the obtained MALDI-TOF MS data highlighted the structural heterogeneity of the polysaccharides studied, and clustered polysaccharide samples with resembling oligosaccharide profiles. Our approach represents a step further towards a generic and accessible identification of plant polysaccharides individually or in a mixture.

1. Introduction

Although plant polysaccharides are the most abundant biomacromolecules found in nature and are frequently used in foods (Harris & Smith, 2006; Saha, Tyagi, Gupta, & Tyagi, 2017), polysaccharide analysis remains slow and laborious. Most approaches currently used to characterize and identify polysaccharides are based on the enzymatic digestion of polysaccharides into structure-informative (diagnostic) oligosaccharides, followed by analysis of the released oligosaccharides (Broxterman, Picouet, & Schols, 2017; Leijdekkers, Huang, Bakx, Gruppen, & Schols, 2015; Remoroza, Broxterman, Gruppen, & Schols, 2014). Such an approach requires the use of for example liquid chromatography coupled to mass spectrometry (LC-MS) (Remoroza et al., 2014) and Matrix-Assisted Laser Desorption Ionization Time-Of-Flight Mass Spectrometry (MALDI-TOF MS) to distinguish polysaccharide samples based on their oligosaccharide profiles (Broxterman et al.,

Abbreviations: ABN, sugar beet arabinan; AC, autoclave; AC121-pOx-PS, periodate-oxidized polysaccharide treated with AC at 121 °C; AC134-pOx-PS, periodate-oxidized polysaccharide treated with AC at 134 °C; AX, arabinoxylan; BWX, birch wood xylan; Cel, cellulose; DHB, 2,5-dihydroxybenzoic acid; DO, degree of oxidation; DO_{Rel}, relative DO; DO_{Theo}, theoretical maximum DO; DP, degree of polymerization; ESI, electron spray ionization; GC, gas chromatography; GGM, guar GM; GM, galactomannan; HCA, hierarchical cluster analysis; HCl, hydrochloric acid; HG, homogalacturonan (lemon pectin); H_n, hexose oligomer; HPAEC-PAD, high-performance anion-exchange chromatography with pulsed amperometric detection; HPLC, high-performance LC; HPSEC-RI, high performance size exclusion chromatography with refractive index detection; IO_4^-, periodate; LBGM, locust bean GM; LC, liquid chromatography; MALDI-TOF MS, Matrix-Assisted Laser Desorption Ionization Time-Of-Flight Mass Spectrometry; MLG, barley mixed-linked β-glucan; MS, mass spectrometry; Mw, molecular weight; *m/z*, mass-to-charge ratio; ox-DP_n, oxidized oligosaccharide cluster region potentially with a DP *n*; PC, principal component; PCA, principal component analysis; P_n, pentose oligomer; pOx-PS, periodate-oxidized PS; PS, polysaccharide; RG-I, potato rhamnogalacturonan type I; RT, room temperature; Rt, retention time; RAX, rye AX; TFA, trifluoroacetic acid; UA, uronic acids; $uHexA_n^m$, methyl-esterified unsaturated GalA-oligomer with *n* GalA units and *m* methyl-esters; UHPLC, ultra-high-performance liquid chromatography; WAX, wheat AX; WS, wheat starch; XG, tamarind seed xyloglucan.

* Corresponding author.
E-mail address: henk.schols@wur.nl (H.A. Schols).

https://doi.org/10.1016/j.carbpol.2022.119685
Received 17 February 2022; Received in revised form 16 May 2022; Accepted 30 May 2022
Available online 1 June 2022

2017; Lerouxel et al., 2002; Westphal, Schols, Voragen, & Gruppen, 2010). Even though enzymatic digestion of polysaccharides is a powerful strategy to obtain diagnostic oligosaccharides, there is not a universal enzyme (mixture) able to release oligosaccharides from all polysaccharides, since enzymes are polysaccharide structure-specific (Lombard, Golaconda Ramulu, Drula, Coutinho, & Henrissat, 2014). Additionally, enzymatic digestion of polysaccharides composed of isomeric sugar units results in oligosaccharides with isomeric structures, which cannot easily be distinguished by MS (Bauer, 2012; Kailemia, Ruhaak, Lebrilla, & Amster, 2014).

Periodate (IO_4^-) oxidation is a potential alternative approach for generating oligosaccharides and overcoming some of the enzymatic digestion limitations. Periodate oxidation of polysaccharides leads to specific oxidation of free vicinal diols to aldehydes with cleavage of the carbon chain (Kristiansen, Potthast, & Christensen, 2010). In aqueous systems, the aldehyde groups of periodate-oxidized polysaccharides can also be present in masked forms (*e.g.* as hydrates, hemiacetals and hemialdals) (Nypelö, Berke, Spirk, & Sirviö, 2021). An attractive feature of periodate oxidation of polysaccharides is that it can also lead to polysaccharide depolymerization, which allows the formation of oligosaccharides. Recently, we demonstrated by using electrospray ionization (ESI-)MS that periodate oxidation of plant polysaccharides releases oligosaccharides that are polysaccharide structure-dependent (Pandeirada, Achterweust, et al., 2022). These oligosaccharides comprised dialdehyde, hemialdal, and hydrated aldehyde structural components, forming highly complex, and highly informative, periodate-oxidized oligosaccharide structures. Unfortunately, it was shown that the optimum conditions for periodate oxidation of plant polysaccharides into oligosaccharides differ per polysaccharide structure (Pandeirada, Achterweust, et al., 2022). This prevented to have a single approach to release oligosaccharides from polysaccharides. A possible solution to reach a polysaccharide depolymerization method based on periodate oxidation that is common to a broad range of polysaccharides could be the inclusion of a subsequent thermal depolymerization treatment. Veelaert, de Wit, Gotlieb, and Verhé (1997) observed an extensive decrease in the molecular weight of a periodate-oxidized starch upon heating (90 °C) in acidic (pH 3 and 5) and neutral conditions. This indicates that subjecting periodate-oxidized polysaccharides to a thermal treatment in an aqueous solution might yield sufficient levels of oligosaccharides that are polysaccharide structure-dependent due to the high specificity of IO_4^- to oxidize vicinal diols (Perlin, 2006).

In this study, we investigate the use of a thermal treatment to depolymerize periodate-oxidized plant polysaccharides into oligosaccharides in a more generic manner than by using enzymes. The thermally depolymerized periodate-oxidized polysaccharides were analysed by MALDI-TOF MS for polysaccharides fingerprinting based on the oligosaccharide MS profiles. Additionally, MALDI-TOF MS data was subjected to principal component analysis (PCA) and hierarchical cluster analysis (HCA) as complementary techniques to substantiate variations among samples and to cluster polysaccharide samples based on the oligosaccharide profiles.

2. Materials and methods

2.1. Materials

Birch wood xylan (BWX), microcrystalline cellulose (Cel), L-(+)-arabinose (Ara, purity 99%), L-(−)-fucose (Fuc, purity 99%), D-(+)-galactose (Gal, purity 97%), D-(+)-glucose (Glc, purity 99%), D-(+)-glucuronic acid (GlcA, purity 98%), and rhamnose monohydrate ($Rha{\cdot}H_2O$, purity 99%) were obtained from Sigma (Darmstadt, Germany). Wheat flour arabinoxylan (WAX; Ara:Xyl = 38:62, purity >95%, medium viscosity), rye flour arabinoxylan (RAX; Ara:Xyl = 38:62, purity ~90%), barley mixed-linked β-glucan (MLG; purity ~95%, low viscosity), potato rhamnogalacturonan type I (RG-I; Purity >90%; GalA:Rha:Ara:Xyl:Gal:Other sugars (%) = 61.0:6.2:2.5:0.5:23.1:6.7), and sugar beet arabinan (ABN; purity ~95%; Ara:Gal:Rha:GalA:Other sugars (%) = 69:18.7:1.4:10.2:0.7) were obtained from Megazyme (Wicklow, Ireland). Guar galactomannan (GGM, Man:Gal = 2:1) was from BFGoodrich Diamalt GmbH (Munich, Germany), locust bean galactomannan (LBGM, Man:Gal = 4:1) from Unipektin (Eschenz, Switzerland), tamarind seed xyloglucan (XG; Gal:Glc:Xyl (%) = 7.9:58.9:33.1 (Table S1)) from Dainippon Sumitomo Pharma Co. Ltd., (Osaka, Japan), and lemon pectin (homogalacturonan — HG with a high degree of methyl-esterification) was from Copenhagen Pectin A/S (Lille Skensved, Denmark). Wheat starch (WS) was obtained from Fluka (Buchs, Switzerland). Sodium metaperiodate ($NaIO_4$, 98%) was purchased from Alfa Aesar (Thermo Fisher, Kandel, Germany). Ethylene glycol, D-(+)-xylose (Xyl), and D-(+)-galacturonic acid monohydrate ($GalA{\cdot}H_2O$, purity 98%) were from Merck (Darmstadt, Germany). LC-MS water was of UHPLC-grade (Biosolve, Valkenswaard, The Netherlands). 2,5-Dihydroxybenzoic acid (DHB) was from Bruker Daltonics (Bremen, Germany). All water was purified in a Milli-Q system from Millipore (Molsheim, France), unless otherwise mentioned.

2.2. Periodate oxidation of polysaccharides

Various arabinoxylan:glucan mixes composed of WAX:MLG (93:7%, w/w), WAX:MLG:WS (65:5:30%, w/w), RAX:MLG (86:14%, w/w), and RAX:MLG:WS (30:5:65%, w/w) were prepared. These mixtures were prepared in the ratio that is commonly found in wheat and rye brans, respectively (Roye et al., 2020). Another polysaccharide mix (PS mix) was composed of WAX:MLG:GGM:HG:RG-I:ABN (1:1:1:1:1:1%, w/w). Mixes and individual polysaccharides (BWX, WAX, RAX, MLG, WS, XG, Cel, GGM, LBGM, HG, RG-I, and ABN) were periodate-oxidized in duplicate. The reaction volume was set at 40 mL, and 200 mg of PS powder was used in all experiments. Polysaccharides were solubilized in (37.6 mL) water 1) under magnetic stirring overnight (xylans, XG, HG, RG-I, ABN), or 2) under vigorous magnetic stirring of the slurry covered with aluminium foil on a hot-plate at 120 °C until boiling, followed by stirring without heat until the PS was fully dissolved (MLG, GMs, and PS mix), or 3) by autoclaving at 121 °C for 20 min (WS, Cel and AX mixes). After PS solubilization, a freshly prepared 250 μmol/mL $NaIO_4$ solution (2.4 mL) was added to the PS solution to reach a 3.0 μmol $NaIO_4$/mg PS ratio. The glass reaction flask was protected from light with aluminium foil, and the reaction was carried out at room temperature (RT) for 6 h, as previously described (Pandeirada, Achterweust, et al., 2022). Periodate-oxidized (pOx-) PS samples were characterized and subjected to a thermal treatment using an autoclave (Section 2.4).

2.3. Sugar composition analysis by HPAEC-PAD

Sugar composition of the pOx-PS samples (BWX, AXs, MLG, LBGM, WS, HG, RG-I, ABN, and AX:glucan mixes (2.0 mg)) was determined after methanolysis (3.0 M HCl in dried methanol, 16 h, 80 °C) and TFA acid hydrolysis (2.0 M, 1 h, 121 °C) as described elsewhere (Pandeirada, Merkx, Janssen, Westphal, & Schols, 2021). Hydrolysates were diluted in water to about 25 μg/mL before analysis. Sugar composition of (pOx-) GGM, XG, Cel and PS mix samples (10 mg) was accessed after pre-hydrolysis for 10 min, or for 1 h for Cel samples, at 30 °C in 72% (w/w) H_2SO_4 followed by hydrolysis for 3 h at 100 °C in 1.0 M H_2SO_4. Sulphuric acid hydrolysates were 100 times diluted with water before analysis. The monosaccharides released were analysed by High-Performance Anion-Exchange Chromatography with Pulsed Amperometric Detection (HPAEC-PAD). An ICS-5000 HPLC system (Dionex, Sunnyvale, CA, USA) equipped with a CarboPac PA1 guard column (2 mm ID × 50 mm) and a CarboPac PA-1 column (2 mm × 250 mm) (Dionex) was used for this analysis. Detection of the eluted compounds was performed by an ED40 EC-detector running in the PAD mode (Dionex). 10 μL of the diluted hydrolysates was injected into the system and compounds were eluted as described previously (Pandeirada et al., 2021). All samples were analysed in duplicate. Monosaccharide

standards (arabinose, xylose, fucose, galactose, glucose, mannose, glucuronic acid, galacturonic acid, and rhamnose) in a concentration range of 1.0–150 μg/mL were used for quantification. The collected data were analysed using Chromeleon 7.2 software (Dionex). The degree of oxidation (DO) (Eq. (1)) of samples was calculated based on the decrease in the sugar recovery relative to the respective native PS or PS mixes. The relative DO (DO_{Rel}) (Eq. (2)) was calculated using the theoretical maximum DO (DO_{Theo}) that each PS can reach, and the calculated DO (Table S1). DO_{Theo} was calculated based on the expected total remaining sugar content, if all sugar units containing vicinal diols are oxidized.

$$\text{DO}\ (\%, \text{w/w}) = 100 - \text{Relative sugar recovery of pOx-PS} \quad (1)$$

$$\text{DO}_{\text{Rel}}\ (\%, \text{w/w}) = \frac{\text{DO}}{\text{DO}_{\text{Theo}}} \times 100 \quad (2)$$

2.4. Thermal depolymerization of periodate oxidized polysaccharides

Two reaction temperatures, 121 and 134 °C, were initially tested for their ability to degrade native and periodate-oxidized BWX, WAX, GGM, XG and HG samples in aqueous solution (1.0 mg/mL). Based on these preliminary experiments, a temperature of 121 °C was selected to further depolymerize all native and periodate-oxidized plant polysaccharides investigated in this study. All native polysaccharides and one replica of each pOx-PS (individuals and mixes) were solubilized in water (1.0 mg/mL) and thermally degraded at 121 °C (in duplicate) in an autoclave (AC) device (Zirbus Technology Benelux B.V., Tiel, The Netherlands) for 20 min at 2300 mbar, yielding AC121-pOx-PS. After AC treatment, part of the AC121(-pOx-)HG/RG-I samples was freeze-dried and analysed for methyl-ester and acetyl content.

2.5. Uronic acid, methyl and acetyl content

Periodate-oxidized and non-oxidized BWX, HG, RG-I, ABN and PS mix were sulphuric acid-hydrolysed as described in Section 2.3, and the total uronic acid content was determined using an automated colorimetric *m*-hydroxydiphenyl method (Blumenkrantz & Asboe-Hansen, 1973; Thibault & JF, 1979).

Periodate-oxidized and non-oxidized HG/RG-I samples before and after AC treatment were saponified in duplicate at 5.0 mg/mL in 0.1 M NaOH for 24 h (1 h at 4 °C followed by 23 h at RT) to hydrolyse methyl-esters. The methanol released was quantified by headspace gas chromatography (GC) analysis as described elsewhere (Huisman, Oosterveld, & Schols, 2004). The collected data were analysed using Xcalibur 4.1 software (Thermo Scientific). After GC analysis, samples were centrifuged (16,000 ×*g*, 10 min) and analysed by HPLC on an Ultimate 3000 system (Dionex) coupled to a Shodex RI-101 detector (Showa Denko K. K., Tokyo, Japan) to determine the acetyl content. The HPLC was equipped with an Aminex HPX-87H Ion exclusion column (300 mm × 7.8 mm) with guard column (30 mm × 4.6 mm), both from BIO-RAD (Hercules, CA, USA). The column oven temperature was maintained at 40 °C during analysis. 20 μL of standard (acetic acid 0.005–2.0 mg/mL) and samples were injected onto the system and eluted with 5.0 mM H_2SO_4 solution at a flow rate of 0.6 mL/min for 30 min. Collected data were analysed using Chromeleon 7.2 software (Dionex).

2.6. Molecular weight distribution by HPSEC-RI

The average molecular weight (Mw) was determined by high performance size exclusion chromatography (HPSEC) on an Ultimate 3000 system (Dionex) coupled to Shodex RI-101 detector (Showa Denko K.K.) as described elsewhere (Pandeirada et al., 2021). Columns were calibrated with pullulan (0.180–708 kDa; Polymer Laboratories, UK) and pectin standards (10–100 kDa, as estimated by viscometry (Deckers, Olieman, Rombouts, & Pilnik, 1986)). Standards and samples were analysed at 1.0 mg/mL. Collected data were analysed using Chromeleon 7.2 software (Dionex). The extent of polysaccharide depolymerization after AC treatment into various degree of polymerization (DP; DP < 2, 2 < DP < 20, DP > 20; as % released per DP_x) was calculated as percentage of the total area of the native PS. For DP < 2, the area under the peak with a retention time (Rt) > 14.7, >14.5, or >14.3 min was used for the treated pentosans, hexosans, or polymers containing uronic acids (HG and RG-I), respectively. For 2 < DP < 20, the area between 12.7 min < Rt < 14.7 min, 12.6 min < Rt < 14.5 min, or 12.0 min < Rt < 14.3 min was used for pentosans, hexosans, or HG and RG-I, respectively. For DP > 20, the area with a Rt < 12.7 min, <12.6 min, or < 12.0 min was used for pentosans, hexosans, or HG and RG-I, respectively.

2.7. Screening of oligosaccharides by Matrix-Assisted Laser Desorption/Ionization Time-Of-Flight Mass Spectrometry (MALDI-TOF MS)

1.0 μL of DHB matrix solution (25 mg/mL DHB in 50% (v/v) acetonitrile/water) was mixed with 1.0 μL of AC121-pOx-PS (1.0 mg/mL) on a MALDI plate (Bruker Daltonics, Bremen, Germany). Then, the MALDI plate was dried under a stream of air. Each AC121-pOx-PS replica was applied onto the MALDI plate at two different spots, giving a total of 4 replicas per AC121-pOx-PS sample. For MALDI-TOF MS analysis, a Bruker — Ultraflextreme MALDI-TOF/TOF-MS (Bruker Daltonics, Bremen, Germany) equipped with a 337 nm laser was used. The mass spectrometer was operated in the positive mode and calibrated with a mixture of maltodextrins (AVEBE, Veendam, The Netherlands; mass range 500–3500 Da). After a delayed extraction time of 120 ns, the ions were accelerated with a 25 kV voltage and subsequently detected using the reflector mode. Measurements were performed in the *m/z* 500–2500 range. The lowest laser intensity that allowed us to obtain a clear spectrum was used, and in total 4 times 250 shots were taken per spot to exclude interferences due to local differences in crystallization. The resulting MALDI-TOF mass spectra from all replicas of each AC121-pOx-PS sample displayed identical magnitude signals. Collected MALDI-TOF MS data were analysed using flexAnalysis 3.3 software (Bruker Daltonics). Repetitive series of oxidized oligosaccharide clusters were observed in the whole MALDI-TOF mass spectrum range analysed, as observed by ESI-MS analysis of periodate-oxidized oligosaccharides in our previous work (Pandeirada et al., 2022a). Therefore, a zoom-in of the *m/z* 800–1200 range of the MALDI-TOF mass spectra of all AC121-pOx-PS and -mixes is shown and discussed in this paper.

2.8. Statistical analysis of MALDI-TOF MS data

The generated MALDI-TOF MS data (the exact *m/z* values and their intensities) were analysed using the R statistical software package (Team, 2017). The *m/z* range between 800 and 1200 was used. The AC121-pOx-XG and AC121-pOx-RG-I samples were not subjected to statistical analysis since their MALDI-TOF mass spectra (*m/z* 800–1200) had a low overall signal intensity (<500). Principal component analysis (PCA) was performed (using the R package FactoMineR (Lê, Josse, & Husson, 2008)) to emphasize the most important variation and create a low dimensional overview of the data in the form of score plots. Hierarchical cluster analysis (HCA), an unsupervised clustering method, will put similar spectra in the same clusters, highlighting samples that display similar oligosaccharide profiles. Prior to PCA and HCA, replicates of MALDI-TOF mass spectra were averaged.

For PCA, all (averaged) spectra were mean centred and unit variance scaled. HCA used Ward's linkage method and a distance criterium based on Pearson's correlation coefficient, which was applied on the MALDI-TOF mass spectra.

A series of two independent sample *t*-tests (using an alpha of 0.05) were used to find significantly different *m/z* values between any two polysaccharide classes of xylans (BWX, WAX, and RAX), glucans (WS and MLG), galactomannans (GGM and LBGM) or pectins (HG and ABN). Furthermore, two independent sample *t*-tests were also used to find significantly different *m/z* values within each of the following

polysaccharide classes: 1) xylans (AC121-pOx-BWX, AC121-pOx-WAX), (AC121-pOx-BWX, AC121-pOx-RAX), and (AC121-pOx-WAX, AC121-pOx-RAX); 2) glucans (AC121-pOx-WS, AC121-pOx-MLG); 3) galactomannans (AC121-pOx-GGM, AC121-pOx-LBGM); and 4) pectins (AC121-pOx-HG, AC121-pOx-ABN). Significances ("*p*-values") were adjusted according to the method of Benjamini and Hochberg (1995) to reduce the risk of false positives.

3. Results and discussion

A single polysaccharide (PS) depolymerization approach based on a combination of periodate oxidation (pOx) and autoclave (AC) treatment was investigated to obtain PS structure-dependent oligosaccharides in a generic manner. The present approach was applied to a broad range of plant polysaccharides that were divided into the following classes: xylans (BWX and AXs), glucans (MLG, WS, XG, and Cel), galactomannans (GMs), and pectic polysaccharides (HG, RG-I, and ABN). Furthermore, AX:MLG(:WS) mixes, and a PS mix composed of WAX:MLG:GGM:HG:RG-I:ABN (1:1:1:1:1:1 ratio (w/w)) were also subjected to the above approach in order to validate our approach for complex mixtures of polysaccharides. The oligosaccharides released were analysed by MALDI-TOF MS to investigate if PS structure-dependent MALDI-TOF MS oligosaccharide profiles are obtained for recognition of the parental polysaccharides.

3.1. Degree of oxidation of periodate-oxidized polysaccharides based on the sugar recovery

All individual plant polysaccharides, AX:MLG(:WS) mixes and the PS mixes were periodate-oxidized at room temperature (RT) for 6 h using a 3.0 μmol $NaIO_4$/mg PS ratio. This periodate oxidation condition was selected since it allows the formation of soluble periodate-oxidized (pOx-)plant polysaccharides with minimal loss of non-sugar substituents and sugar side chains. In addition, under this periodate oxidation condition, pOx-polysaccharides are expected to be obtained with a relative degree of oxidation (DO_{Rel}) 40 < DO_{Rel} < 80% and low formation of side oxidation products (Pandeirada, Achterweust, et al., 2022). In addition, this oxidation condition was selected because partial PS oxidation already allows the formation of oligosaccharides that are PS structure-dependent.

Regarding individual pOx-PS samples, xylans were obtained with a DO_{Rel} of 39, 74, and 93% (w/w) for pOx-BWX, pOx-RAX, and pOx-WAX, respectively (Table S1). This shows that AXs are more easily oxidized than BWX, as previously reported (Pandeirada, Achterweust, et al., 2022), and that although WAX and RAX have an identical Ara:Xyl ratio, pOx-WAX had a higher DO_{rel} than pOx-RAX. This might be due to different levels of single- and double-substitution levels of the Xyl units between WAX and RAX (Pandeirada, Speranza, et al., 2022). WAX is more double substituted than RAX, whereas RAX is more single substituted than WAX. This suggests that an AX containing more double-substituted Xyl units might be more easily oxidized since it also contains a higher level of unsubstituted Xyl units. Additionally, the different DO_{Rel} between WAX and RAX might also be due to different Ara (and/or [Me]GlcA) residue distributions over the xylan backbone (Bromley et al., 2013; Gruppen, Hamer, & Voragen, 1992; Izydorczyk, 2009). For glucans, pOx-MLG and pOx-WS had a DO_{rel} > 90%, whereas pOx-XG displayed a DO_{rel} ~ 35%, which was due to (almost) complete oxidation/degradation of the Gal and Xyl side chains. Cel did not undergo oxidation at all, most likely due to its insolubility hindering any noticeable periodate oxidation (Perlin, 2006).

pOx-GGM and pOx-LBGM samples had a DO_{rel} of 80 and 72%, respectively, with all the Gal side chains of both GMs completely oxidized and/or partially removed. This shows that the side chains are more readily oxidized than the Man units in the backbone, in accordance with literature (da Silva et al., 2020; Pandeirada, Speranza, et al., 2022). Regarding pectic polysaccharides, pOx-HG, pOx-RG-I, and pOx-ABN displayed a DO_{rel} of 39, 76, and 98%, respectively (Table S1). None of the Rha and Glc units initially present in the native ABN and RG-I samples were recovered in the respective pOx-ABN and pOx-RG-I samples, indicating that these sugar units were fully oxidized and/or degraded. Nonetheless, still some Ara, Gal, and uronic acid (UA) units initially present in ABN were recovered in pOx-ABN, and some Gal and UA units of RG-I were recovered in pOx-RG-I. Altogether, these results show that overoxidation (DO_{Rel} > 100%) of individual polysaccharides did not occur, which is important to preserve a structure still closely related to the native PS structure.

Regarding PS mixes, pOx-WAX:MLG and pOx-WAX:MLG:WS had a DO_{Rel} of 80 and 72%, respectively, and pOx-RAX:MLG and pOx-RAX:MLG:WS had a DO_{Rel} of 71 and 77%, respectively. The pOx-PS mix had a DO_{Rel} of 68%. In all pOx-AX:glucan mixes, Ara, Xyl and Glc units were still detected (Table S1), confirming that full or overoxidation of the polysaccharides present in the mix also did not occur. Furthermore, the DO_{Rel} obtained for the studied PS mixes were overall lower than the DO_{Rel} obtained for each individual PS when oxidized separately. This suggests that periodate oxidation of individual polysaccharides is influenced by the presence of other polysaccharides. Yet, a DO_{Rel} between 68 and 80% could be obtained for PS mixes, indicating that at least partial oxidation of all polysaccharides has occurred, which is important to further release PS-specific oligosaccharides.

3.2. Preliminary thermal treatment of periodate-oxidized polysaccharides

pOx-BWX, pOx-WAX, pOx-GGM, pOx-XG, and pOx-HG were thermally treated at 121 and 134 °C for 20 min using AC, resulting in AC121-pOx-PS and AC134-pOx-PS samples, respectively. All samples were analysed for oligomers released using HPSEC (results only shown for 121 °C treatment in the following paragraph). AC121-pOx-PS samples displayed molecules with a degree of polymerization (DP) from 2 to 20, except AC121-pOx-XG, which still exhibited a high molecular weight (Mw). Increasing the AC temperature to 134 °C boosted the release of the remaining non-oxidized Ara side chains of pOx-WAX (HPAEC data not shown), and it did not further increase the degradation of pOx-GGM and pOx-XG as judged from HPSEC. For pOx-HG, AC treatment at 134 °C increased the degradation comparatively to the treatment at 121 °C, and mainly released additional monomers and enhanced the release of methyl-esters. AC121-pOx-HG recovered approx. 54% (w/w native HG) methyl-esters, whereas AC134-pOx-HG only recovered approx. 27% methyl-esters.

Based on these preliminary results, an AC treatment at 121 °C was selected to study the degradation of all the different pOx-PS samples and pOx-PS mixes. At this temperature it is expected that all studied pOx-plant polysaccharides, except (pOx-)XG, will be depolymerized to oligosaccharides with minimal loss of structural features. As Cel did not undergo oxidation and due to its insolubility, (pOx-)Cel was not further subjected to AC treatment.

3.3. Molecular weight distribution of thermally treated pOx-PS samples

The Mw distribution of the native and pOx-PS samples before and after AC treatment at 121 °C was analysed by HPSEC (Fig. S1, Xylans; Fig. S2, Glucans; Fig. S3, AX-Glucan mixes; Fig. S4, GMs; Fig. S5, Pectins; and Fig. S6, PS mix), and the extent of PS depolymerization is shown in Table 1. None or only minor changes in the Mw distribution were observed for all native polysaccharides and mixes after AC treatment. On the contrary, all AC121-pOx-PS and -mixes had molecular weights lower than the respective pOx-PS, corroborating that the Mw of pOx-PS samples in aqueous solutions decreases upon heating (Veelaert et al., 1997). Furthermore, all AC121-pOx-PS samples, except AC121-pOx-XG, comprised oligosaccharides (35 to 79%; 2 < DP < 20; Table 1). This result highlights that periodate oxidation of plant polysaccharides at RT for 6 h using a 3.0 μ$NaIO_4$/mg PS followed by an AC treatment at 121 °C is a promising approach to depolymerize plant polysaccharides into

Table 1
Percentage of periodate-oxidized (pOx-) polysaccharide (PS) depolymerized into the various degree of polymerization (DP) segments DP < 2, 2 < DP < 20 (oligosaccharide range), and DP > 20, before and after autoclave (AC) treatment at 121 °C (AC121).

Sample	Percentage[a] of depolymerized polymer into various DP		
	DP < 2	2 < DP < 20	DP > 20
pOx-BWX*	1.2	26.8	44.3
AC121-pOx-BWX	5.3 ± 0.6	41.8 ± 1.1	65.0 ± 2.7
pOx-WAX*	2.0	49.6	38.5
AC121-pOx-WAX	4.4 ± 0.0	49.9 ± 2.2	14.5 ± 2.0
pOx-RAX*	2.1	36.1	53.0
AC121-pOx-RAX	4.3 ± 0.7	40.2 ± 1.1	24.2 ± 2.3
pOx-MLG*	0.7	37.2	22.5
AC121-pOx-MLG	2.1 ± 0.5	37.2 ± 1.8	15.4 ± 0.5
pOx-WS[b]*	31.1	148.7	11.6
AC121-pOx-WS[b]	49.3 ± 0.4	74.0 ± 1.2	33.9 ± 0.1
pOx-XG[c]	Insoluble sample		
AC121-pOx-XG[d]	0.0 ± 0.0	2.9 ± 0.4	27.6 ± 3.3
pOx-WAX:MLG*	1.7	44.6	47.3
AC121-pOx-WAX:MLG	5.2 ± 1.4	59.6 ± 0.1	36.3 ± 9.9
pOx-WAX:MLG:WS*	3.4	49.7	61.0
AC121-pOx-WAX:MLG:WS	5.7 ± 1.6	55.2 ± 5.7	34.0 ± 0.4
pOx-RAX:MLG*	1.6	28.7	53.4
AC121-pOx-RAX:MLG	4.2 ± 0.3	41.8 ± 0.5	29.7 ± 0.3
pOx-RAX:MLG:WS[b]*	4.9	65.7	165.7[b]
AC121-pOx-RAX:MLG:WS[b]	12.9 ± 2.3	79.1 ± 7.4	144.1 ± 4.0[b]
pOx-GGM*	2.8	24.6	62.4
AC121-pOx-GGM	10.7 ± 0.1	35.8 ± 0.9	32.9 ± 0.4
pOx-LBGM*	9.9	63.5	31.4
AC121-pOx-LBGM	17.7 ± 0.3	43.5 ± 0.1	4.4 ± 0.3
pOx-HG*	0.0	2.4	93.2
AC121-pOx-HG	7.5 ± 0.4	67.0 ± 1.8	4.8 ± 0.2
pOx-RG-I*	0.0	21.2	51.9
AC121-pOx-RG-I	5.2 ± 0.2	45.2 ± 3.1	15.4 ± 2.2
pOx-ABN*	0.0	4.6	90.1
AC121-pOx-ABN	3.6 ± 0.5	44.5 ± 3.2	27.6 ± 1.4
pOx-PS mix*	0.0	11.1	88.8
AC121-pOx-PS mix	4.8 ± 0.1	51.6 ± 0.8	38.8 ± 2.9

[a] Results are expressed as average (n = 2) of the area percentage (%) relative to the total area of the respective untreated native polysaccharide as described in Section 2.6.
[b] Samples solubility increased after AC treatment and/or periodate oxidation.
[c] Model became insoluble after periodate oxidation.
[d] Sample contained some insoluble material.
* Single sample used to perform the AC121 treatment is shown.

oligosaccharides in a generic manner. This overcomes the requirement to have specific enzymes per structurally different PS when using an enzymatic depolymerization approach.

3.4. MALDI-TOF MS analysis of thermally treated pOx-PS

The Mw distribution results showed that all AC121-pOx-PS, except AC121-pOx-XG, and -mixes released oligosaccharides. Particularly for AC121-pOx-HG and AC121-pOx-RG-I, some loss of ester groups (methyl-esters and acetyl groups; Fig. S7) occurred during periodate oxidation and AC treatment. Despite this, the oligosaccharide profiles of the AC121-pOx-PS samples and -mixes might still be sufficiently PS structure-dependent.

All individual AC121-pOx-PS samples that contained oligosaccharides comprised clusters of oxidized oligosaccharides, except AC121-pOx-RG-I (Fig. 1–5), in their MALDI-TOF mass spectra, confirming our previous work on the ESI-MS analysis of periodate-oxidized plant polysaccharides (da Silva et al., 2020; Pandeirada, Achterweust, et al., 2022). In the present work, we decided to use MALDI-TOF MS over ESI-MS because it is a quicker and more straight forward technique and during our previous research we observed that MALDI-TOF MS spectra and direct infusion ESI-Ion trap-MS provided the same information (Pandeirada et al., 2022a; results not shown). Clusters of oxidized oligosaccharide fragments are marked as **ox-DP$_n$** (oxidized oligosaccharide cluster region potentially with a DP n) in the MALDI-TOF mass spectra (Fig. 1-5). Each **ox-DP$_n$** region is composed of various sub-oligosaccharide clusters that comprise various m/z values that were Δ −(x + n * 2) Da relative to the corresponding DP-oligomer or, particularly for AC121-pOx-WS and AC121-pOx-HG, relative to the corresponding highest DP-oxidized oligomer within the **ox-DP$_n$** cluster, where x = 12–214 and n = 0–4. The n * 2 is due to variable levels (n) of dialdehydes. The x is due to various oxidation reactions that can take place during periodate oxidation, such as double oxidations, intramolecular cleavages of an (oxidized) sugar unit, and hemialdals formation, or even due to a combination of these reactions, as explained before (da Silva et al., 2020; Pandeirada, Achterweust, et al., 2022). In principle this high variety of oxidized oligosaccharide structures is attractive as it would increase the likelihood of obtaining unique patterns for identification. Below, the MALDI-TOF mass spectra (m/z 800–1200) of the various AC121-pOx-PS and -mixes will be compared and discussed.

3.4.1. Xylans

The MALDI-TOF mass spectrum of AC121-pOx-BWX (Fig. 1A) showed that each **ox-DP$_n$** region comprised the following sub-oligosaccharide clusters: Δ −(18 + n * 2), Δ −(60 + n * 2), and Δ −(76 + n * 2) Da, with n = 0, 1 and 2, relative to the corresponding pentose-oligomer (P_n). The sub-oligosaccharide cluster P_n Δ −(76 + n * 2) Da was always the major sub-oligosaccharide cluster of each **ox-DP$_n$** in AC121-pOx-BWX.

Both AXs, AC121-pOx-WAX and AC121-pOx-RAX, comprised the same **ox-DP$_n$** regions, which were formed by the sub-oligosaccharide clusters Δ −(44 + n * 2), Δ −(60 + n * 2), and Δ −(76 + n * 2), with n = 0–4, relative to P_n (Fig. 1B and C). Notably, the sub-cluster P_n Δ −(18 + n * 2) Da present in AC121-pOx-BWX was absent in the spectra of both AC121-pOx-AXs, while the latter displayed the sub-cluster P_n Δ −(44 + n * 2) Da as an additional sub-oligosaccharide cluster. This highlights that a moderately substituted xylan with UA (<10%, w/w; Table S1) (BWX) and AXs generate oxidized oligosaccharide profiles that are PS structure-dependent after periodate oxidation and AC treatment. Remarkably, the ions m/z 919 and 1051 of the sub-clusters P_n Δ −(44 + n * 2) Da of AC121-pOx-AXs (Fig. 1B and C) were significantly different from AC121-pOx-BWX (p < 0.05). Hence, these m/z values can be considered marker oligosaccharides for AXs, allowing us to distinguish them from BWX.

Although the **ox-DP$_n$** regions of AC121-pOx-WAX and AC121-pOx-RAX comprised the same sub-oligosaccharide clusters (Fig. 1B and C), their proportion within each **ox-DP$_n$** region varied between WAX and RAX. For AC121-pOx-WAX, the sub-oligosaccharide cluster P_n Δ −(60 + n * 2) Da was the principal sub-oligosaccharide cluster in each **ox-DP$_n$** cluster, followed by the sub-oligosaccharide cluster P_n Δ −(76 + n * 2) Da (Fig. 1B). While for AC121-pOx-RAX (Fig. 1C), both sub-oligosaccharide clusters P_n Δ −(60 + n * 2) Da and P_n Δ −(76 + n * 2) Da were similarly present in each **ox-DP$_n$**. These results highlight that although both WAX and RAX display an identical Ara:Xyl ratio, their differences in the Ara distribution along the xylan backbone (Pandeirada, Speranza, et al., 2022) leads to differences in the proportion of oxidized oligosaccharides released from pOx-AXs after AC treatment at 121 °C. This result is highly relevant because it shows that even the same type of PS derived from different sources having only slightly different structures can be distinguished using our approach.

3.4.2. Glucans

Regarding glucans, two **ox-DP$_n$** regions (ox-DP_6 and ox-DP_7) could be well-defined for AC121-pOx-MLG (Fig. 1D). For AC121-pOx-WS, only one **ox-DP$_n$** region (ox-$DP_{6/7}$) that comprised oxidized oligosaccharides derived from a DP 6 and/or DP 7 was defined (Fig. 1E). The given **ox-DP$_n$** cluster for AC121-pOx-WS was considered as one cluster since repetitive throughout the entire MALDI-TOF MS range (m/z 500–2500) analysed (data not shown). Notably, none of the sub-oligosaccharide

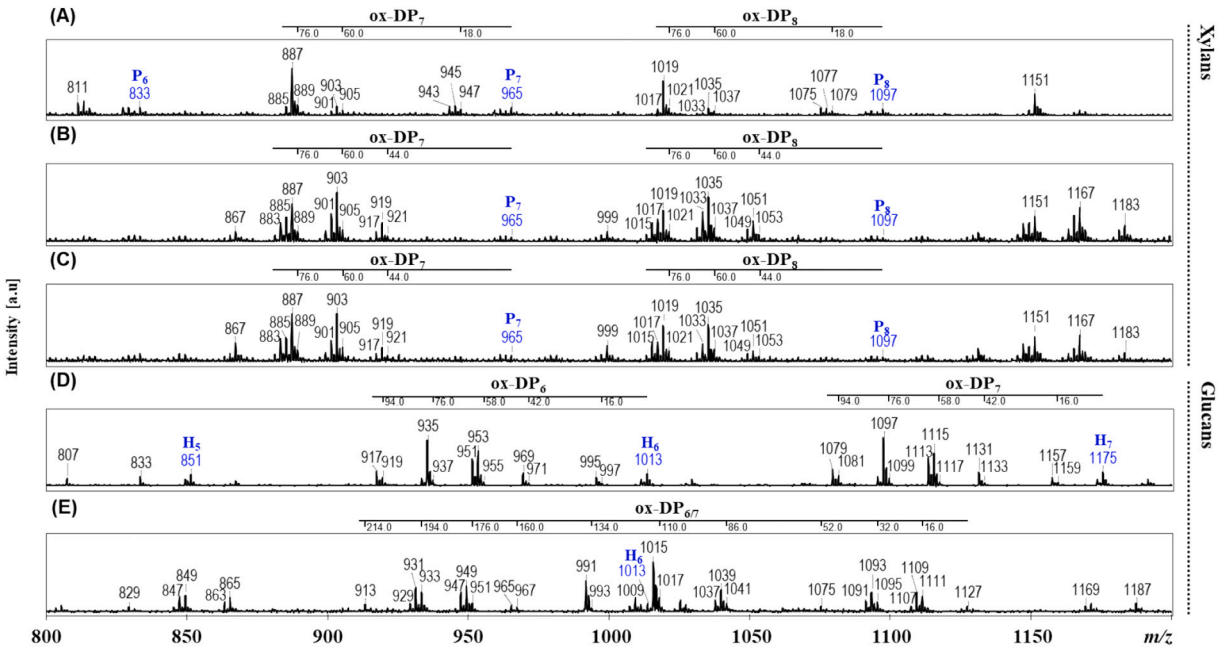

Fig. 1. MALDI-TOF mass spectra (*m/z* 800–1200 range) of the AC121 treated periodate-oxidized BWX (**A**), WAX (**B**), RAX (**C**), MLG (**D**), and WS (**E**). $\mathbf{P_n}$ or $\mathbf{H_n}$ — Na^+ adduct of an oligomer composed of n pentoses (Ara or Xyl) or hexoses (Glc). **ox-DP$_n$** — *m/z* region of a cluster of oxidized oligosaccharides potentially with a n DP. *m/z* differences from each sub-oligosaccharide cluster with Δ −(x + *n* * 2) Da, *n* = 0–4, to the corresponding non-oxidized DP-oligomer are depicted in (A–D). In (E), *m/z* differences from each sub-oligosaccharide cluster with Δ −(x + *n* * 2) Da, *n* = 0–3, are given in relation to the highest oxidized *m/z* value detected within the **ox-DP$_n$** cluster. Detected non-oxidized oligomers are highlighted in blue.

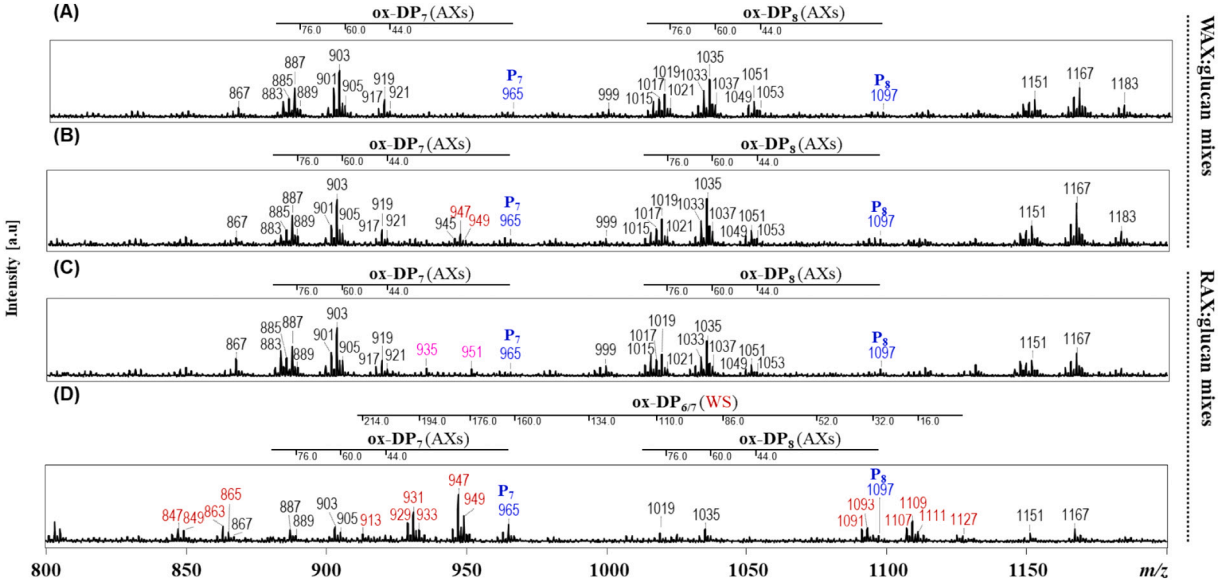

Fig. 2. MALDI-TOF mass spectra (*m/z* 800–1200 range) of the AC121 treated periodate-oxidized WAX:MLG (93:7%, *w*/w; **A**), WAX:MLG:WS (65:5:30%, w/w; **B**), RAX:MLG (86:14%, w/w; **C**), and RAX:MLG:WS (30:5:65%, w/w; **D**). $\mathbf{P_n}$ or $\mathbf{H_n}$ — Na^+ adduct of an oligomer composed of n pentoses (Ara or Xyl) or hexoses (Glc). **ox-DP$_n$** (AXs) — *m/z* region of a cluster of oxidized oligosaccharides derived from AXs potentially with a n DP. **ox-DP$_n$** (WS) — *m/z* region of a cluster of oxidized oligosaccharides derived from WS potentially with a n DP. Detected non-oxidized oligomers are highlighted in blue, and oxidized oligomers derived from AXs, MLG, and WS are highlighted in black, pink, and red, respectively.

clusters present in the MALDI-TOF mass spectra of both glucans coincided, showing that different oligosaccharide profiles are obtained between samples. Hence, various significantly different ($p < 0.05$) *m/z* values were found for MLG (*m/z* 1097, 1115, and 1157) and for WS (*m/z* 913, 931, 949, 965, 991, 1015, 1039, 1075, 1093, 1109, 1127, and 1169), acting as marker oligosaccharides for the corresponding glucan.

3.4.3. AX:MLG(:WS) mixes

To investigate whether the main cereal hemicellulose components (AXs and MLG) can be identified when present in a mix based on the MALDI-TOF MS oligosaccharide profiles derived from AC121-pOx-PS samples, AX:MLG mixes were prepared in the proportion that are found in wheat and rye brans (Roye et al., 2020). An AX:MLG:WS mix was also prepared because starch is also present in cereal bran preparations. While the oligosaccharide pattern of AC121-pOx-WAX:MLG

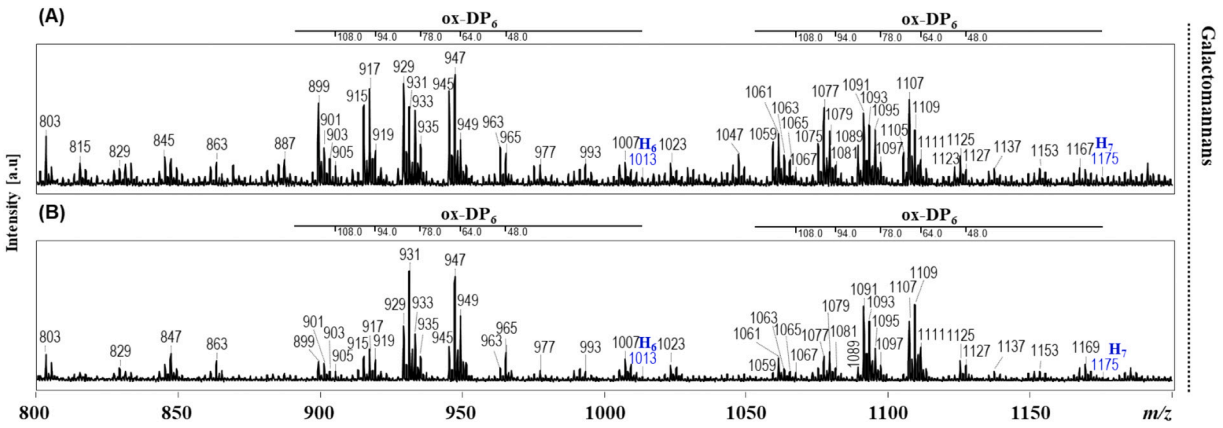

Fig. 3. MALDI-TOF mass spectra (*m/z* 800–1200 range) of the AC121 treated periodate-oxidized GGM (**A**) and LBGM (**B**). $\mathbf{H_n}$ — Na^+ adduct of an oligomer composed of n hexoses (Gal and/or Man). $\mathbf{ox\text{-}DP_n}$ — *m/z* region of a cluster of oxidized oligosaccharides potentially with a n DP. *m/z* differences from each sub-oligosaccharide cluster with Δ −(x + *n* * 2) Da, *n* = 0–4, to the corresponding non-oxidized DP-oligomer are depicted. Detected non-oxidized oligomers are highlighted in blue.

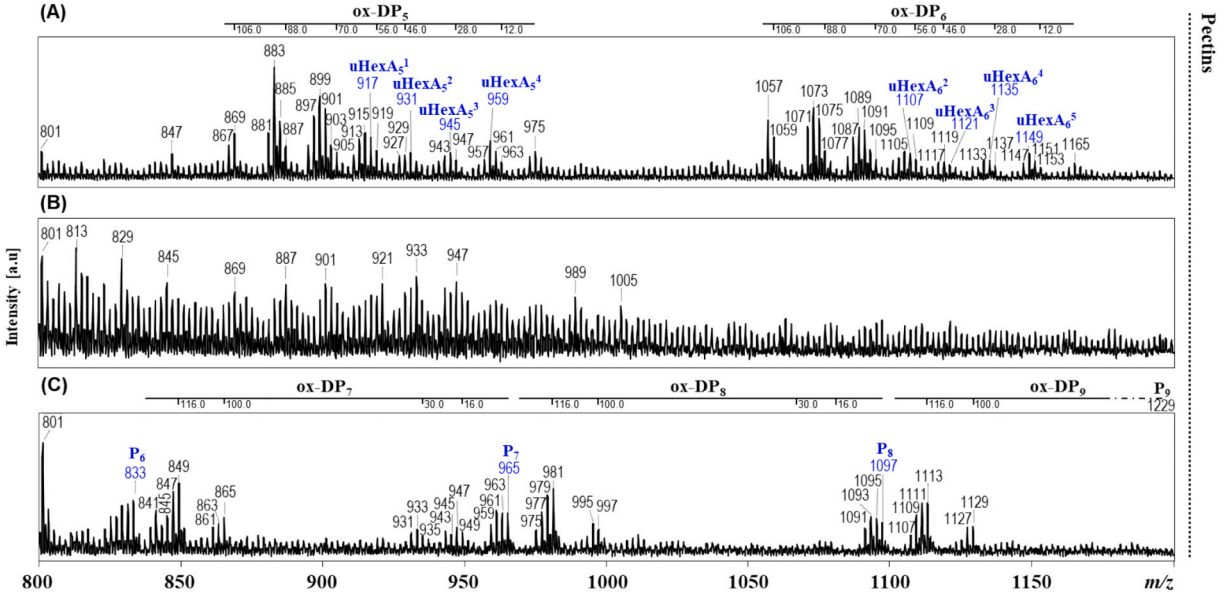

Fig. 4. MALDI-TOF mass spectra (*m/z* 800–1200 range) of the AC121 treated periodate-oxidized HG (**A**), RG-I (**B**), and ABN (**C**). $\mathbf{uHexA_n^m}$ — Oligomer composed of n GalA units from which one is unsaturated and m methyl-esters. $\mathbf{P_n}$ — Na^+ adduct of an oligomer composed of n pentoses (Ara). $\mathbf{ox\text{-}DP_n}$ *m/z* region of a cluster of oxidized oligosaccharides potentially with a n DP. In (**A**), *m/z* differences from each sub-oligosaccharide cluster with Δ −(x + *n* * 2) Da, *n* = 0–5, are given in relation the highest oxidized *m/z* value detected within the $\mathbf{ox\text{-}DP_n}$ cluster. In (B), $\mathbf{ox\text{-}DP_n}$ regions could not be defined for RG-I. In (C), *m/z* differences from each sub-oligosaccharide cluster with Δ −(x + *n* * 2) Da, *n* = 0–4, to the corresponding non-oxidized DP-oligomer are depicted. Detected non-oxidized oligomers are highlighted in blue.

(93:7%, w/w) (Fig. 2A) was the same as AC121-pOx-WAX (Fig. 1B), the one of AC121-pOx-WAX:MLG:WS (65:5:30%, w/w) (Fig. 2B) additionally comprised minor levels of WS-oxidized oligosaccharides. This shows that the mass spectra of AC121-pOx-WAX:MLG(:WS) 'bran' mixes are dominated by AX-oxidized oligosaccharides.

The AC121-pOx-RAX:MLG (86:14%, w/w) (Fig. 2C) also displayed an oligosaccharide pattern identical to the individual AC121-pOx-RAX (Fig. 1C), with negligible amounts of MLG-oxidized oligosaccharides. On the contrary, AC121-pOx-RAX:MLG:WS (30:5:65%, w/w) comprised RAX- and WS-oxidized oligosaccharides (Fig. 2D). In this RAX:MLG:WS mix, WS accounted for 65% of the mix, whereas in the WAX:MLG:WS mix, WS represented 30%. The higher proportion of WS in the rye mix compared to the wheat mix might explain the additional presence of WS-oxidized oligosaccharides in the MALDI-TOF mass spectrum of AC121-pOx-RAX:MLG:WS mix besides AX-oxidized oligosaccharides. This suggests that the release of periodate-oxidized oligosaccharides derived from different polysaccharides when present in a mix depends on the proportion of each PS in the mix. This can explain why MLG-oxidized oligosaccharides were not detected in the mass spectra of the AC121-pOx-AX:MLG(:WS) mixes with a MLG proportion < 10%. Yet, these results highlight that periodate oxidation/AC treatment of products containing wheat and/or rye bran hemicellulose components, followed by analysis of the oligosaccharides released by MALDI-TOF MS, has potential to identify AXs, regardless the presence of MLG and/or WS.

3.4.4. Galactomannans

The MALDI-TOF mass spectra of both AC121-pOx-GGM and AC121-pOx-LBGM (Fig. 3A and B) displayed the same oxidized oligosaccharide clusters. However, the proportion of sub-oligosaccharide clusters that formed the $\mathbf{ox\text{-}DP_n}$ region of each AC121-pOx-GM differed. 4 sub-oligosaccharide clusters, namely H_n Δ -(64 + *n* * 2), H_n Δ -(78 + *n* * 2), H_n Δ -(94 + *n* * 2), and H_n Δ -(108 + *n* * 2) Da, were predominantly

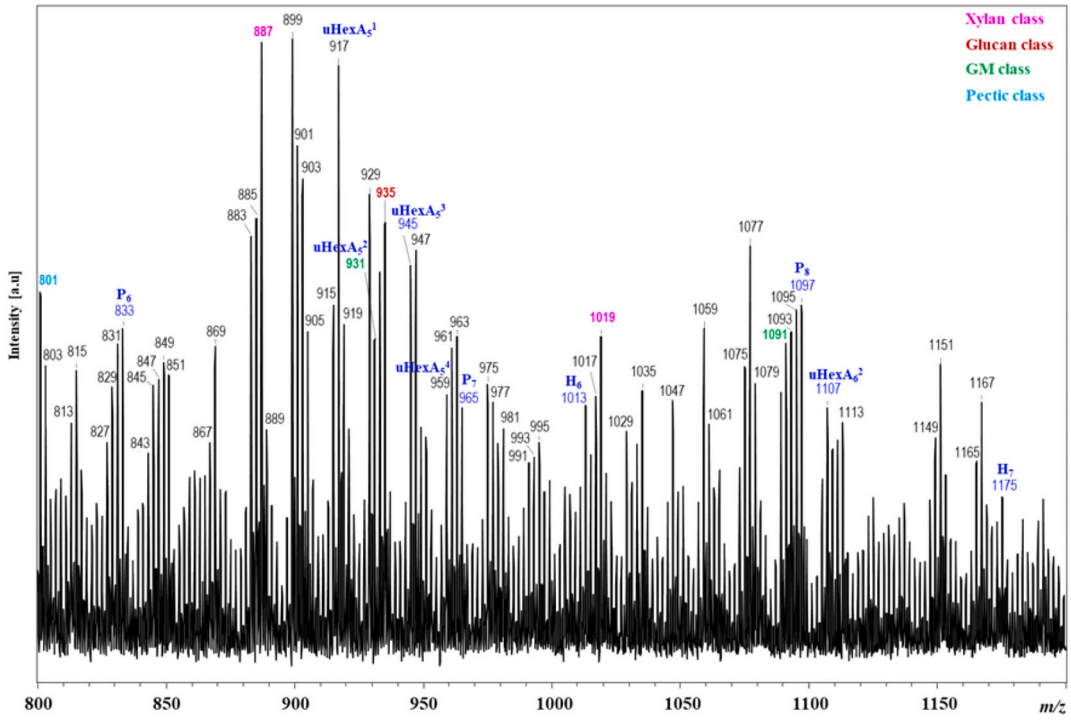

Fig. 5. MALDI-TOF mass spectra (*m/z* 800–1200 range) of the AC121 treated periodate-oxidized PS mix (WAX:MLG:GGM:HG:RD-I:ABN 1:1:1:1:1:1:1 ratio (w/w)). $\mathbf{P_n}$ or $\mathbf{H_n}$ — Na^+ adduct of an oligomer composed of n pentoses (Ara or Xyl) or hexoses (Glc, Gal, and/or Man); $\mathbf{uHexA_n^m}$ — oligomer composed of n GalA units from which one is unsaturated and m methyl-esters. Detected non-oxidized oligomers are highlighted in dark blue. Significantly different ($p < 0.05$) *m/z* values found for the xylan, glucan, GM, and pectic polysaccharides class between PS classes are highlighted in pink, red, green, and light blue, respectively.

present in each $\mathbf{ox\text{-}DP_n}$ region of AC121-pOx-GGM (Fig. 3A). In AC121-pOx-LBGM, the last 2 sub-oligosaccharide clusters of each $\mathbf{ox\text{-}DP_n}$ (H_n Δ -(108 + *n* * 2) and H_n Δ -(94 + *n* * 2)) were present in much lower abundance than the precedent 2 sub-oligosaccharide clusters (H_n Δ -(64 + *n* * 2) and H_n Δ -(78 + *n* * 2); Fig. 3B). In addition, the ions *m/z* 899, 917, 1061 and 1077 were significantly more abundant ($p < 0.05$) in AC121-pOx-GGM than in AC121-pOx-LBGM. Therefore, these *m/z* values were considered marker oligosaccharides of GGM, allowing us to distinguish GGM from LBGM. The MALDI-TOF MS results obtained for galactomannans, glucans, and (arabino)xylans are particularly interesting because they show that periodate oxidation/AC treatment of structurally different polysaccharides composed of isomeric sugar units generates unique oligosaccharide profiles.

3.4.5. Pectins

Regarding pectic polysaccharides (Fig. 4A–C), AC121-pOx-HG displayed two $\mathbf{ox\text{-}DP_n}$ regions in the *m/z* 800–1200 range (Fig. 4A). Within these $\mathbf{ox\text{-}DP_n}$ regions, HG-oxidized and methyl-esterified unsaturated GalA-oligomers ($uHexA_n^m$) were identified. This result highlights that some contiguous GalA segments that were partially methyl-esterified resisted periodate oxidation and were further cleaved by AC treatment. Additionally, the presence of unsaturated sugar units indicates that an AC treatment degrades a pOx-HG *via* a β-elimination reaction (Veelaert et al., 1997).

For AC121-pOx-RG-I, many oligosaccharides were obtained (Fig. 4B). However, these oligosaccharides had a very low signal abundance throughout the entire mass spectrum range shown, not exhibiting any clear pattern of clusters of oxidized oligosaccharides. In contrast, AC121-pOx-ABN comprised three $\mathbf{ox\text{-}DP_n}$ clusters (Fig. 4C) that were totally different from the $\mathbf{ox\text{-}DP_n}$ regions of AC121-pOx-HG (Fig. 4A). Therefore, some significantly ($p < 0.05$) different *m/z* values were found for AC121-pOx-ABN (*m/z* 849, 865, 981, 995, 1113, and 1129) and for AC121-pOx-HG (*m/z* 883, 915, 1057, and 1089), and were considered marker oligosaccharides between both these samples. These results show that also AC121-pOx-pectic elements generate PS structure-dependent MS oligosaccharide profiles. Remarkably, MALDI-TOF MS oligosaccharide profiles of Ara-based polymer AC121-pOx-ABN (Fig. 4C) was also different from the ones obtained for the xylans investigated (Fig. 1A–C).

3.4.6. PS mix (WAX:MLG:GGM:HG:RG-I:ABN)

A PS mix composed of WAX:MLG:GGM:HG:RG-I:ABN in an 1:1:1:1:1:1:1 ratio (w/w) was also periodate-oxidized and AC treated to investigate if different PS classes can be identified when present in a complex mixture of polysaccharides. The MALDI-TOF mass spectrum of the AC121-pOx-PS mix (Fig. 5) exhibited *m/z* values derived from all individual AC121-pOx-PS samples (Fig. 1B, 1D, 3A, 4A–C). Despite being rather complex, the mass spectrum of AC121-pOx-PS mix still allowed us to get hints on the type of polysaccharides present in the mixture. Statistical analysis of the spectra between the various (AC121-pOx-)PS classes using a *t*-test with $p < 0.05$ showed that 1) the oligosaccharides with *m/z* 887 and 1019 were significantly more abundant in the xylan class than in all the other studied PS classes; 2) the oligosaccharides with *m/z* 931, 947, 1091 and 1107 were significantly more abundant in GMs than in xylans and pectic polysaccharides; 3) the ion *m/z* 935 was significantly more abundant in glucans than in xylans and pectic polysaccharides, whereas the oligosaccharides with *m/z* 1013 was more significantly abundant in glucans than in GMs; and 4) the ion *m/z* 801 was most significantly abundant in pectic polysaccharides. Detection of some of these marker *m/z* values per PS class in the MALDI-TOF mass spectrum of the AC121-pOx-PS mix (Fig. 5) allowed us to unambiguously recognize the presence of pectic (*m/z* 801), GM (*m/z* 931 and 1091), glucan (*m/z* 935), and xylan components (*m/z* 887 and 1019).

Our results show that periodate oxidation/AC treatment of plant polysaccharides and -mixes is a potential approach to depolymerize polysaccharides in a generic manner, releasing oligosaccharides that are PS structure-dependent. This result is of the outmost importance since it highlights that purified plant polysaccharides and plant polysaccharides

present in complex mixes can be identified based on their unique MALDI-TOF MS oligosaccharide profiles. It should be noted that in a PS mix, if a PS is present in a proportion lower than 10%, it might escape identification since no detectable oligosaccharides might be observed in the MALDI-TOF mass spectrum.

3.5. Exploratory PCA and HCA analysis of MALDI-TOF mass spectra of thermally treated pOx-PS samples

To illustrate and emphasize sources of variations among MALDI-TOF MS oligosaccharide profiles of AC121-pOx-PS and -mixes, and to cluster PS samples with similar oligosaccharide profiles, principal component analysis (PCA) and hierarchical cluster analysis (HCA) were performed.

The first two principal components (PC1 and PC2) of the PCA (Fig. 6A) accounted for 71.4% of the total variance, with PC1 explaining most of the variation (57.9%). AC121-pOx-MLG and AC121-pOx-WS samples were separated along PC1, which might be due to completely different MS oligosaccharide profiles for these samples (Fig. 1). Individual polysaccharides within the xylan-, GM- and pectin classes were separated along PC2. Notably, PCA also confirmed that the Ara-based polymer (AC121-pOx-)ABN was not closely related to any other pentose-based xylan polymer. Hence, PCA of the MALDI-TOF MS data clearly stressed the structural differences of all polysaccharides investigated in this study, even between the same type of polysaccharides (*e.g.* WAX *vs* RAX, and GGM *vs* LBGM).

MALDI-TOF MS results indicated that the oligosaccharide profiles of AC121-pOx-WAX:MLG(:WS) and AC121-pOx-RAX:MLG were comparable to the respective AC121-pOx-AX, whereas the mass spectrum of AC121-pOx-RAX:MLG:WS displayed both RAX- and WS-oxidized oligosaccharides. Although AC121-pOx-AX:MLG and AC121-pOx-AX:MLG:WS mixes were grouped together in the PCA (Fig. 6A), these samples were separated from AC121-pOx-AX and AC121-pOx-WS. This was not obvious from the MALDI-TOF MS results, indicating that there is distinct difference between AC121-pOx-AX:glucan mixes and the individual AC121-pOx-polysaccharides.

The correlation-based distance dendrogram obtained from HCA (Fig. 6B) clustered xylans in branch **a2** and GMs in branch **b5** (Fig. 6B), whereas the other PS classes (glucans and pectins) were not clustered. AC121-pOx-WAX and AC121-pOx-RAX were closer to each other than to AC121-pOx-BWX. In addition, the dendrogram highlighted that AC121-pOx-RAX:MLG:WS was more intimately correlated to AC121-pOx-WS (branch **b**, Fig. 6B) than to AC121-pOx-RAX (branch **a**, Fig. 6B), confirming the MALDI-TOF MS results (Fig. 2D). Altogether, MALDI-TOF MS analysis of the AC121-pOx-PS samples studied combined with advanced data sciences methods such as PCA and HCA highlighted that our proposed method has potential to distinguish and identify PS within a specific PS class, and to identify different PS classes in a mixture. In addition, polysaccharides with resembling MALDI-TOF MS oligosaccharide profiles after periodate oxidation and AC treatment could be clustered.

4. Conclusions

In this study, depolymerization of periodate-oxidized plant polysaccharides and polysaccharide (PS) mixes using an autoclave (AC) treatment at 121 °C was an approach investigated to release oligosaccharides for polysaccharides fingerprinting. All investigated plant polysaccharides were depolymerized releasing oligosaccharides, except xyloglucan. MALDI-TOF MS analysis of the oligosaccharides released showed that structure-dependent oligosaccharide profiles were obtained per PS. This allowed us to distinguish even between polysaccharides with resembling structures, such as birch wood xylan *vs* wheat arabinoxylan *vs* rye arabinoxylan, and guar galactomannan *vs* locust bean galactomannan. Furthermore, based on significantly different ($p < 0.05$) marker *m/z* values identified per PS class, also different PS classes could be detected in the MALDI-TOF mass spectrum of a complex PS mix. These results bring us a step closer to recognize different polysaccharides and/or PS classes using a single PS depolymerization approach. The approach proposed could be extended to other food polysaccharides to create a MALDI-TOF MS data library. Later on, this approach should also be applied to a real food matrix in order to verify and validate if the created MALDI-TOF MS data library allows us to recognize individual polysaccharides in a food product more easily. In addition, to clearly demonstrate the heterogeneity within and between PS classes, and cluster polysaccharides with resembling MS oligosaccharide profiles, performing PCA and HCA on the MALDI-TOF MS data is a nice complementary approach. Thus, periodate oxidation of plant PS followed by an AC treatment and MALDI-TOF MS analysis is a promising

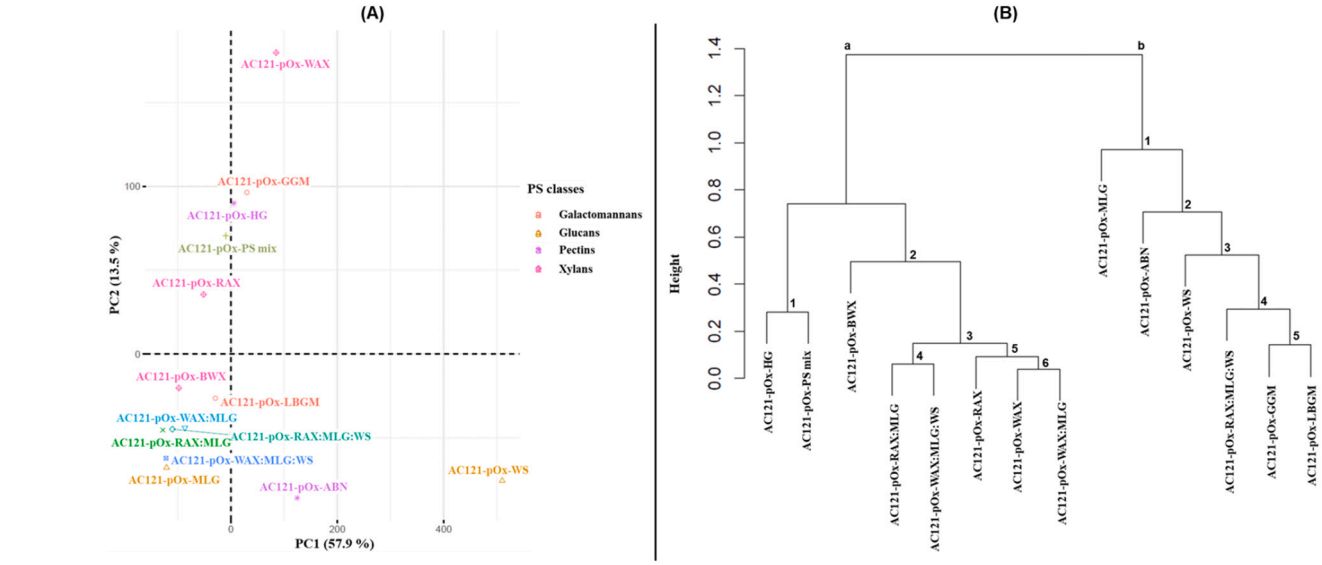

Fig. 6. (**A**) Principal component analysis (PCA) biplot, and (**B**) hierarchical cluster analysis (HCA) represented as a correlation-based distance dendrogram constructed with the MALDI-TOF mass spectra data (*m/z* 800–1200) of the various periodate-oxidized (pOx-) samples degraded using an AC treatment at 121 °C (AC121-pOx-BWX, AC121-pOx-WAX, AC121-pOx-RAX, AC121-pOx-MLG, AC121-pOx-WS, AC121-pOx-GGM, AC121-pOx-LBGM, AC121-pOx-HG, AC121-pOx-ABN, AC121-pOx-AX:MLG(:WS), and AC121-pOx-PS mix). The PCA scores were plotted for PC1 and PC2, and the amount of variance explained by each PC is shown in parentheses.

approach to depolymerize polysaccharides into PS-specific oligosaccharides in a more generic manner than by using enzymes.

CRediT authorship contribution statement

Carolina O. Pandeirada: Conceptualization, Methodology, Investigation, Data curation, Writing – original draft, Writing – review & editing. **Jos A. Hageman:** Formal analysis, Data curation, Writing – review & editing. **Hans-Gerd Janssen:** Conceptualization, Methodology, Writing – review & editing. **Yvonne Westphal:** Conceptualization, Methodology, Writing – review & editing. **Henk A. Schols:** Conceptualization, Methodology, Writing – review & editing.

Declaration of competing interest

The authors declare that they have no known competing financial interests or personal relationships that could have appeared to influence the work reported in this paper.

Appendix A. Supplementary data

Supplementary data to this article can be found online at https://doi.org/10.1016/j.carbpol.2022.119685.

References

Bauer, S. (2012). Mass spectrometry for characterizing plant cell wall polysaccharides. *Frontiers in Plant Science, 3*(45). https://doi.org/10.3389/fpls.2012.00045

Benjamini, Y., & Hochberg, Y. (1995). Controlling the false discovery rate: A practical and powerful approach to multiple testing. *Journal of the Royal Statistical Society: Series B (Methodological), 57*(1), 289–300. https://doi.org/10.1111/j.2517-6161.1995.tb02031.x

Blumenkrantz, N., & Asboe-Hansen, G. (1973). New method for quantitative determination of uronic acids. *Analytical Biochemistry, 54*(2), 484–489. https://doi.org/10.1016/0003-2697(73)90377-1

Bromley, J. R., Busse-Wicher, M., Tryfona, T., Mortimer, J. C., Zhang, Z., Brown, D. M., & Dupree, P. (2013). GUX1 and GUX2 glucuronyltransferases decorate distinct domains of glucuronoxylan with different substitution patterns. *The Plant Journal, 74*(3), 423–434. https://doi.org/10.1111/tpj.12135

Broxterman, S. E., Picouet, P., & Schols, H. A. (2017). Acetylated pectins in raw and heat processed carrots. *Carbohydrate Polymers, 177*, 58–66. https://doi.org/10.1016/j.carbpol.2017.08.118

da Silva, L. M., Araújo, L. F. S., Alvez, R. C., Ono, L., Sá, D. A. T., da Cunha, P. L. R., Monteiro de Paula, R. C., & Maciel, J. S. (2020). Promising alternative gum: Extraction, characterization, and oxidation of the galactomannan of Cassia fistula. *International Journal of Biological Macromolecules, 165*, 436–444. https://doi.org/10.1016/j.ijbiomac.2020.09.164

Deckers, H. A., Olieman, C., Rombouts, F. M., & Pilnik, W. (1986). Calibration and application of high-performance size exclusion columns for molecular weight distribution of pectins. *Carbohydrate Polymers, 6*(5), 361–378. https://doi.org/10.1016/0144-8617(86)90026-3

Gruppen, H., Hamer, R. J., & Voragen, A. G. J. (1992). Water-unextractable cell wall material from wheat flour. 2. Fractionation of alkali-extracted polymers and comparison with water-extractable arabinoxylans. *Journal of Cereal Science, 16*(1), 53–67. https://doi.org/10.1016/S0733-5210(09)80079-9

Harris, P. J., & Smith, B. G. (2006). Plant cell walls and cell-wall polysaccharides: Structures, properties and uses in food products. *International Journal of Food Science and Technology, 41*(Suppl. 2), 129–143. https://doi.org/10.1111/j.1365-2621.2006.01470.x

Huisman, M. M. H., Oosterveld, A., & Schols, H. A. (2004). Fast determination of the degree of methyl esterification of pectins by head-space GC. *Food Hydrocolloids, 18*(4), 665–668. https://doi.org/10.1016/j.foodhyd.2003.11.006

Izydorczyk, M. S. (2009). 23 - arabinoxylans. In G. O. Phillips, & P. A. Williams (Eds.), *Handbook of hydrocolloids* (2nd ed., pp. 653–692). Woodhead Publishing.

Kailemia, M. J., Ruhaak, L. R., Lebrilla, C. B., & Amster, I. J. (2014). Oligosaccharide analysis by mass spectrometry: A review of recent developments. *Analytical Chemistry, 86*(1), 196–212. https://doi.org/10.1021/ac403969n

Kristiansen, K. A., Potthast, A., & Christensen, B. E. (2010). Periodate oxidation of polysaccharides for modification of chemical and physical properties. *Carbohydrate Research, 345*(10), 1264–1271. https://doi.org/10.1016/j.carres.2010.02.011

Lê, S., Josse, J., & Husson, F. (2008). FactoMineR: An R package for multivariate analysis. *Journal of Statistical Software, 25*(1), 1–18. https://doi.org/10.18637/jss.v025.i01

Leijdekkers, A. G. M., Huang, J. H., Bakx, E. J., Gruppen, H., & Schols, H. A. (2015). Identification of novel isomeric pectic oligosaccharides using hydrophilic interaction chromatography coupled to traveling-wave ion mobility mass spectrometry. *Carbohydrate Research, 404*, 1–8. https://doi.org/10.1016/j.carres.2014.12.003

Lerouxel, O., Siang Choo, T., Séveno, M., Usadel, B., Faye, L., Lerouge, P., & Pauly, M. (2002). Rapid structural phenotyping of plant cell wall mutants by enzymatic oligosaccharide fingerprinting. *Plant Physiology, 130*(4), 1754–1763. https://doi.org/10.1104/pp.011965

Lombard, V., Golaconda Ramulu, H., Drula, E., Coutinho, P. M., & Henrissat, B. (2014). The carbohydrate-active enzymes database (CAZy) in 2013. *Nucleic Acids Research, 42*(D1), D490–D495. https://doi.org/10.1093/nar/gkt1178

Nypelö, T., Berke, B., Spirk, S., & Sirviö, J. A. (2021). Review: Periodate oxidation of wood polysaccharides—Modulation of hierarchies. *Carbohydrate Polymers, 252*. https://doi.org/10.1016/j.carbpol.2020.117105

Pandeirada, C. O., Achterweust, M., Janssen, H.-G., Westphal, Y., & Schols, H. A. (2022a). Periodate oxidation of plant polysaccharides provides polysaccharide-specific oligosaccharides. *Carbohydrate Polymers, 291*, Article 119540. https://doi.org/10.1016/j.carbpol.2022.119540

Pandeirada, C. O., Merkx, D. W. H., Janssen, H.-G., Westphal, Y., & Schols, H. A. (2021). TEMPO/NaClO2/NaOCl oxidation of arabinoxylans. *Carbohydrate Polymers, 259*, Article 117781. https://doi.org/10.1016/j.carbpol.2021.117781

Pandeirada, C. O., Speranza, S., Bakx, E., Westphal, Y., Janssen, H.-G., & Schols, H. A. (2022b). Partial acid-hydrolysis of TEMPO-oxidized arabinoxylans generates arabinoxylan-structure resembling oligosaccharides. *Carbohydrate Polymers, 276*, Article 118795. https://doi.org/10.1016/j.carbpol.2021.118795

Perlin, A. S. (2006). Glycol-cleavage oxidation. *Advances in Carbohydrate Chemistry and Biochemistry, 60*, 183–250. https://doi.org/10.1016/S0065-2318(06)60005-X

Remoroza, C., Broxterman, S., Gruppen, H., & Schols, H. A. (2014). Two-step enzymatic fingerprinting of sugar beet pectin. *Carbohydrate Polymers, 108*(1), 338–347. https://doi.org/10.1016/j.carbpol.2014.02.052

Roye, C., Bulckaen, K., De Bondt, Y., Liberloo, I., Van De Walle, D., Dewettinck, K., & Courtin, C. M. (2020). Side-by-side comparison of composition and structural properties of wheat, rye, oat, and maize bran and their impact on in vitro fermentability. *Cereal Chemistry, 97*(1), 20–33. https://doi.org/10.1002/cche.10213

Saha, A., Tyagi, S., Gupta, R. K., & Tyagi, Y. K. (2017). Natural gums of plant origin as edible coatings for food industry applications. *Critical Reviews in Biotechnology, 37*(8), 959–973. https://doi.org/10.1080/07388551.2017.1286449

Team, R. C. (2017). R: A language and environment for statistical computing. Retrieved from https://www.R-project.org/.

Thibault, J., & JF, T. (1979). *Automatisation du dosage des substances pectiques par la méthode au métahydroxydiphényl*.

Veelaert, S., de Wit, D., Gotlieb, K. F., & Verhé, R. (1997). Chemical and physical transitions of periodate oxidized potato starch in water. *Carbohydrate Polymers, 33*(2), 153–162. https://doi.org/10.1016/S0144-8617(97)00046-5

Westphal, Y., Schols, H. A., Voragen, A. G. J., & Gruppen, H. (2010). MALDI-TOF MS and CE-LIF fingerprinting of plant cell wall polysaccharide digests as a screening tool for arabidopsis cell wall mutants. *Journal of Agricultural and Food Chemistry, 58*(8), 4644–4652. https://doi.org/10.1021/jf100283b